NON-DIAPHRAGM ELECTRODEPOSITION OF ANTIMONY: EFFECT OF PROCESS PARAMETERS AND PRECIPITATING AGENTS

M.H. Morcali [a*], Ö. Küçükoğlu [b,c], B.N. Çetiner [b], S. Aktaş [b]

[a] Naci Topcuoglu Vocational High School, Gaziantep University, Gaziantep, Turkey
[b] Department of Metallurgy and Materials Engineering, Marmara University, Istanbul, Turkey
[c] Beykent University, Vocational School, Mechanics Department, Esenyurt/İstanbul, Turkey

Abstract

Metallic antimony production from antimony-bearing materials is a research hotspot. The conventional electrowinning technology of antimony is a challenging problem due to the sulfur compounds that come from both the ore itself and the leaching solution in the electrolysis system. The electro-production of antimony in modified non-diaphragm cells is of interest because of the high price and maintenance issues associated with diaphragm cells.
A sulfur-based problem in non-diaphragm cells was the focus of this study, which investigated the effects of various salts on this problem and also optimized antimony production conditions. Various salts (i.e., $BaCl_2$, $CaCl_2$, $Ba(OH)_2$, $Ca(OH)_2$) were used as a precipitating agent for the formation of insoluble salts ($BaSO_4/CaSO_4$ and $BaSO_3/CaSO_3$). Sb concentration, amount of NaOH and Na_2S in the bath, electrowinning time, and temperature were investigated to optimize reaction parameters. The Taguchi experimental design was used to determine the effect of each factor on the Sb deposition. The phases and structures formed during electroproduction were identified with the help of various measurement techniques. This study found that in the presence of 96 mM $BaCl_2$, 45 g/L of Sb concentration, 100 g/L of NaOH, and 60 g/L of Na_2S were the most suitable factors. It was found that 40 ºC was the optimal electrowinning temperature. This result also demonstrated that increasing concentrations of $BaCl_2$ reduced specific energy consumption.

Keywords: Antimony; Electrochemical process; Metallic salts; Precipitation

1. Introduction

As a significant key non-ferrous metal, antimony plays an important and leading role in the development of flame retardant materials; it is also used as an alloying metal in lead alloys, in lead-acid batteries, as a catalyst and stabilizer in plastics fabrication, and as an additive in glass and ceramics. Until recently, antimony has been found in over 100 different mineral species, but stibnite (Sb_2S_3) has been accepted as the principal ore mineral. Owing to the availability of a crisis for the whole of the industries, all raw materials, even when not classed as critical, can be more necessary for a sustainable world economy [1]. The term 'critical materials/metals' is used, preferably when it comes to raw materials heavily dependent on imports and minerals. Up to now, the EU and the USA have included antimony as critical metal in their list. Right now, the EU and the USA get most of this mineral from China and Russia that control more than 80 percent of the world's antimony production. Antimony has not been added to

the list of Brazil and Japan [1-4]. Being one of the critical raw materials on the EU's list, around 43% of antimony (in the form of antimony trioxide) is employed in the manufacturing of flame retardants. Another important usage area of the metalloid, accounting for about 32% of global antimony utilization, is the alloying of lead metal for bearing hard-lead alloys in the manufacture of lead-acid batteries [5-7]. Other usage areas are the fabrication of low-load bearings used in the automotive sector, in addition to the assembling manufacture of household and decorative items such as teapots, vases, and lamp stands. Additionally, tin-lead-antimony solders are utilized broadly in the electronics industry.

The use of antimony can be investigated in four sections: semiconductor manufacturing, high-capacity batteries, critical minerals, and pharmaceuticals. According to published studies of antimony for strategic technologies and sectors in the world. Antimony will play a key role in achieving a more sustainable future powered by renewable energy. For these reasons, to supply high grade Sb_2O_3 or other

Corresponding author: hakanmorcali@gmail.com

compounds of antimony, the metallic antimony production process should be investigated and/or re-designed with environmentally friendly and straightforward updates [6, 8].

Up to now, the extraction of metallic antimony has been carried out in both pyrometallurgical and hydro-electrochemical processes [8-10]. The principle production process of metallic antimony is the pyrometallurgical method that contains roasting and subsequently direct reduction steps. Due to the high producing cost along with the implementation of more strict environmental rules by the governments, hydro-electrochemical technology is more popular than others. However, the hydrometallurgical process is to be reasonable if ore contains precious metals. For example, Sunshine Mining Co. used a similar method to separate valuable metals from antimony [9].

Even though there are some applications based on molten salt and acidic media electrolysis of antimony [11, 12], conventional processes are carried out in alkaline media because of the selective dissolution of antimony [10, 13-16]. According to the alkaline-based hydrometallurgical process, stibnite ore is leached by the combination of sodium sulfide (Na_2S) and sodium hydroxide (NaOH) for the selective dissolution of antimony. The residue of the leaching process contains a high quantity of precious metals such as gold and silver. Metallic antimony can be produced from the filtered antimony-rich solution by electrolysis. Interestingly, nowadays electro-production of antimony has been preferred over the low-grade antimony ore [16]. For instance, J.C. Jiménez-Lugos et al. [17] recovered metallic antimony from spent lead-acid battery terminals through metallurgical process.

The industrial electro-production of antimony uses diaphragm-cell electrolysis including at the Sunshine Mining Co. The diaphragm-cell electrolysis is specific electrolysis that separates the electrolyte into two parts, i.e., the anolyte and the catholyte [18]. During the electro-production of antimony, sulfur is oxidized in several stages and forms polysulfides, sulfates, sulfides, and thiosulfate. This reduces the antimony deposition efficiency. Thus, the diaphragm is used to prevent these sulfur species from migrating toward the cathode surface [6, 8]. However, recent research focuses on non-diaphragm cell electrolysis because of the high maintenance cost of diaphragm-cell electrolysis. The first non-diaphragm cell electrolysis process was patented in 1940 by Holmes [19]. The barium ions were precipitated as the oxidized sulfur species in the form of barium sulfate in the bath. Afterwards, the first industrial application on the barium salt was carried out by Sunshine Mining Co. in 1942. In this process, the soluble barium salts (e.g. $BaCl_2$) could be used to remove the oxidized sulfur species during antimony electro-deposition. However, the process was initially carried out in diaphragm-cell electrolysis.

The first non-diaphragm cell electrolysis of antimony from an alkaline sulfide solution was introduced by Lindstrom [20]. The SO_4^{2-} anions that occurred during electrolysis on the anode surface reacted with Na^+ cations to form a saturated Na_2SO_4 solution. The excess Na_2SO_4 was precipitated and removed from the solution to overcome the decreasing current efficiency caused by sulfur oxidation. However, this process was not sufficient because of the formation of polysulfides and thiosulphates due to low current efficiency [21]. The other electrochemically antimony production from alkaline sulfide solution using non-diaphragm cell electrolysis was conducted by Anderson, Nordwick [9]. According to this process, leached antimony was crystallized and re-dissolved in NaOH solution to remove the sulfur species from the solution. This process is useful in removing sulfur species, but an extra precipitation step is still required for the process. A recent study on metallic antimony production with non-diaphragm cell electrolysis from alkaline sulfur solution was studied by Awe and Sandström [21]. In that study, the oxidation of sulfur ions was prevented by increasing the anode current density, which preferably led to oxygen evolution instead of the oxidation of sulfur ions. Around 90% of the cathode current efficiency was obtained using 10 M NaOH.

When the salt chloride is used as precipitating agents in order to precipitate sulfur species in the bath, the accumulated chloride ions in the bath could be removed from the solution using a reverse osmosis filtration system after repeated electrodeposition. The reverse osmosis filtration system is a cost-effective solution to provide plenty of chlorine-free drinking water for a household. The chloride ions are captured in the Granular Activated Carbon (GAC) filter in the filtration system.

As summarized from the literature, diaphragm cells are used to prevent the oxidized ions from migrating towards the cathode side, but the high cost and maintenance problems of diaphragm electrolysis cells were observed. The effect of various salts ($BaCl_2$, $CaCl_2$, $Ba(OH)_2$, $Ca(OH)_2$) in the non-diaphragm bath was studied here. According to this process, various salts were used as precipitating agents for the formation of $MeSO_4$ and $MeSO_3$ (i.e., Me: Ba^{+2} or Ca^{+2}) salts to overcome the detrimental effect of the oxidized sulfur ions. Additionally, Sb concentration, amount of NaOH and Na_2S quantity in the bath, electrowinning time, and temperature were investigated. The Taguchi experimental design was used to understand the effect of each factor on the Sb deposition.
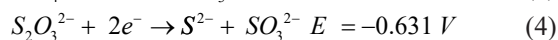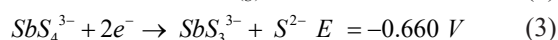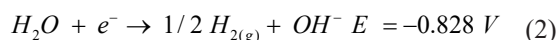
2. Theoretical Background

The primary cathodic reaction for the antimony

electrodeposition process from alkaline sulfide solution is shown in equation 1.

$$SbS_3^{-3} + 3e^- \rightarrow Sb^\circ + 3S^{-2} \quad E = -0.900 \ V \quad (1)$$
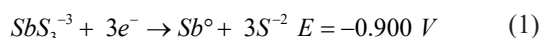
As in all electrometallurgical processes, the main reason for the decrease in efficiency is the undesired side reactions that takes place instead of equation 1. Some of the major undesired side reactions that reduce the electrolysis efficiency are given in equations 2-4.
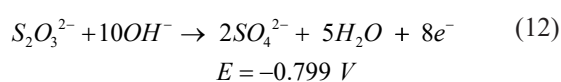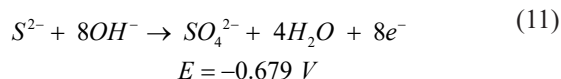
$$H_2O + e^- \rightarrow 1/2 \ H_{2(g)} + OH^- \quad E = -0.828 \ V \quad (2)$$

$$SbS_4^{3-} + 2e^- \rightarrow SbS_3^{3-} + S^{2-} \quad E = -0.660 \ V \quad (3)$$

$$S_2O_3^{2-} + 2e^- \rightarrow S^{2-} + SO_3^{2-} \quad E = -0.631 \ V \quad (4)$$
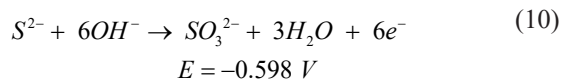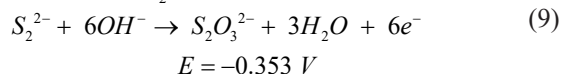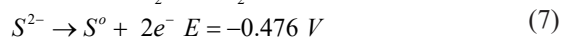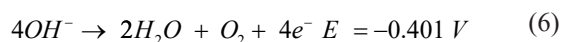
The hydrogen gas formation reaction is the common undesired reaction of all electrodeposition processes. Equation 2 shows the formation of hydrogen gas for alkaline solutions. Fortunately, this reaction can be inhibited when the Sb concentration in the solution is more than 20 g/L [21]. Another undesired side-reaction that causes unnecessary energy consumption on the cathode surface is the reduction reaction of Sb (V) to Sb (III), shown in equation 3. Pentavalent Sb in solution is formed by the oxidation of trivalent Sb by thiosulfates according to equation 5 [6].

$$S_2O_3^{2-} + SbS_3^{3-} \rightarrow SbS_4^{3-} + SO_3^{2-} \quad (5)$$
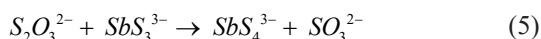
As a result, the thiosulfate formed during the electrolysis is directly responsible for the undesired cathodic reaction indicated in equation 4 and indirectly responsible for the undesired cathodic reaction indicated in equation 3.

The main oxidation reactions occurring at the anode, including the formation of thiosulfate, which reduces the yield in antimony electrolysis, are represented in equations 6 -12.

$$4OH^- \rightarrow 2H_2O + O_2 + 4e^- \quad E = -0.401 \ V \quad (6)$$

$$S^{2-} \rightarrow S^o + 2e^- \quad E = -0.476 \ V \quad (7)$$

$$S^{2-} + S^o \rightarrow S_2^{2-} \quad (8)$$

$$S_2^{2-} + 6OH^- \rightarrow S_2O_3^{2-} + 3H_2O + 6e^- \quad (9)$$
$$E = -0.353 \ V$$

$$S^{2-} + 6OH^- \rightarrow SO_3^{2-} + 3H_2O + 6e^- \quad (10)$$
$$E = -0.598 \ V$$

$$S^{2-} + 8OH^- \rightarrow SO_4^{2-} + 4H_2O + 8e^- \quad (11)$$
$$E = -0.679 \ V$$

$$S_2O_3^{2-} + 10OH^- \rightarrow 2SO_4^{2-} + 5H_2O + 8e^- \quad (12)$$
$$E = -0.799 \ V$$

Equation 6 describes the typical oxygen gas evolution reaction in alkaline solutions. It is the desired reaction since there is no oxidation of sulfur. On the other hand, thiosulfate formation is indicated in equation 9. Here, thiosulfate is formed by the oxidation of polysulfide as shown in equations 7 and 8. Other anodic reactions, which are not preferred to occur thermodynamically due to their low oxidation potentials, are shown in equations 10, 11 and 12. Since these reactions do not contribute to the formation of thiosulfate, they increase the efficiency of antimony electrodeposition. Awe et al. reported that the increase in the anodic current density causes these reactions to occur preferentially, which does not contribute to the formation of thiosulfate. In this study, a new method to prevent the formation of thiosulfate is proposed. Decreasing the sulfate and sulfide concentrations in the solution increases the oxidation potentials of equations 10, 11, and 12, which allows these reactions to occur thermodynamically. In order to reduce the concentration of sulfate and sulfite, the cation that forms insoluble compounds with sulfate and sulfide is added to the electrolyte.

In addition, our hypothesis can be supported by Le Chatelier's principle. The overall reaction of the electrolysis process is given in equation 13. According to Le Chatelier's principle, a decrease in sulfate concentration causes the reaction to proceed to the right.
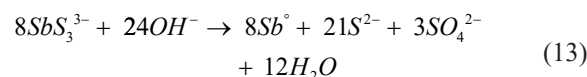
$$8SbS_3^{3-} + 24OH^- \rightarrow 8Sb^\circ + 21S^{2-} + 3SO_4^{2-}$$
$$+ 12H_2O \quad (13)$$

Fig. 1 shows that sulfur is more stable in the form of SO_4^{2-} in alkaline media, which oxidizes Sb (III) to Sb (V).

There are two main approaches to overcoming the problem of antimony.

The first is to prevent the migration of oxidized sulfur to the cathode side, which is diaphragm cell
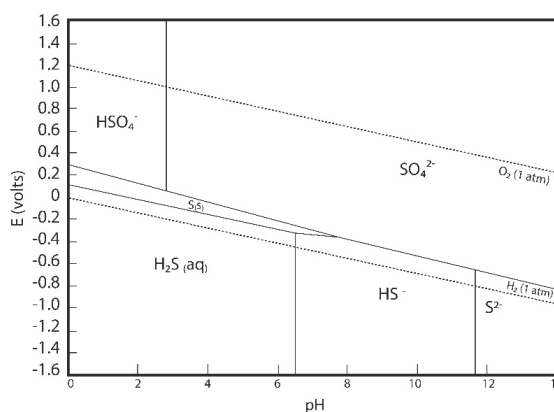

Figure 1. The Eh–pH diagram for the S-H₂O system collected from FactSage Program 6.3 [22]

electrolysis. In this method, an oxidized sulfur species accumulates only on the anolyte side of the electrolyte because of the diaphragm of the cell. Thus, an oxidized sulfur-free catholyte is obtained.

The second approach is to prevent the oxidation of sulfur by increasing the anodic current density. In this method, oxygen evolution becomes more favorable than sulfur. Preventing the oxidation of the sulfur inhibits the undesired antimony oxidation, which increases the Sb deposition efficiency. A higher amount of NaOH present in the solution ensures oxygen evolution.

3. Materials and Methods

Antimony (III) oxide (Sb_2O_3) was used as an antimony source (CAS Number: 1309-64-4 and Product No. 1.07836). Table 1 shows the chemical assay of the purchased material.

Table 1. *The chemical assay of Antimony (III) oxide*

Parameters	Specification (%)
Assay (bromometric)	>99.0
As	<0.03
Ca	<0.002
Cu	<0.002
Fe	<0.003
K	<0.002
Na	<0.002
Pb	<0.025

The first step of the experimental procedure was the leaching of Sb_2O_3 in the combination of Na_2S and NaOH solutions. For example, an alkaline sulfide solution was prepared by dissolving 15 g of NaOH

pellets in 1L distilled water followed by the addition of 50 g of Na_2S flakes. Afterwards, an 30 g of Sb_2O_3 (i.e. 15 g/L of Sb^{3+}) was added to the leaching solution at room temperature and the mixture was mechanically / magnetically stirred for 15 minutes for the complete digestion of Sb_2O_3. The suspension was filtered, and the filtrate was used for the electrodeposition studies. Electro-deposition experiments were conducted in 100 mL borosilicate beakers. Being inert in alkaline solutions, 316 stainless steel plates were used as both the anode and the cathode. The experimental setup is given in Fig. 2.

Before starting the experiment, the initial weight of the electrode (i.e., cathode) was recorded, and the necessary amount of precipitating agent salt was added to the electrolyte solution. The concentrations of the precipitating agents were chosen as mM (millimolar). For all experiments, the distance between electrodes was held at 1 cm via a custom-designed cap containing a doubled slit, and electrodes were connected to a power supply (Unit UTP3315TFL) for electrochemical experiments. A digital multi-meter, Unit UT 181A True RMS, as well as a data-logger, were used to monitor the change in voltage of the electrolysis cell; the current output was checked with a higher precision amp meter. Only 30 cm^2 of the marked electrodes were immersed in the electrolyte to obtain 47.6 A/m^2 and 95.2 A/m^2 current densities, respectively. All experiments were initiated after the electrolyte reached the desired temperature. The temperature was adjusted with a hot plate and measured with a thermometer. The magnetic stirrer was used to mix the electrolyte.

After completing the electro-deposition process, the cathode was rinsed with distilled water to remove the spent electrolyte from the surface of the electrode (See Fig.3). After the cleaning process, the Sb-coated cathode was dried in a drying oven for 4 hrs. at 100 °C. The weight of the Sb-coated cathode was measured to five decimal points to ascertain the quantity of the accumulated antimony on the cathode surface.
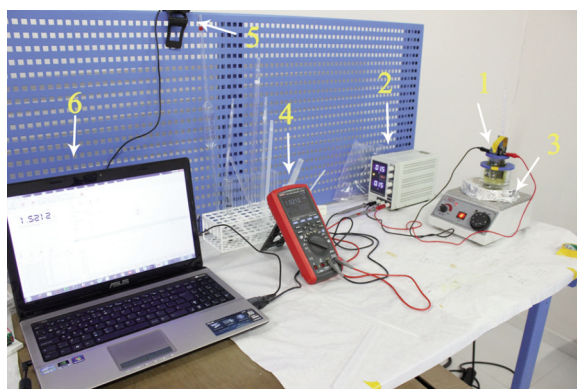

Figure 2. *The Experimental setup (1.The electrolysis cell; 2.The power supply; 3.The magnetic stirrer; 4.Data-logger; 5.Camera for recording experiments; 6.Computer connected with the data-logger to record data during the experiment)*
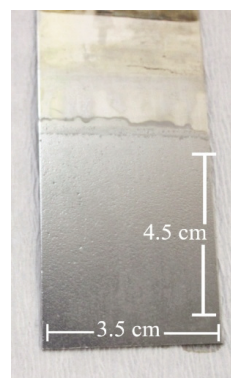

Figure 3. *The picture of Electrodeposited Antimony on the cathode*

The spent electrolyte was then filtered, and the antimony concentration remaining in the solution was determined by Atomic Absorption Spectrometry (AAS); the produced antimony sponge was characterized by X-ray Fluorescence (XRF), X-ray Diffraction (XRD), and Scanning Electron Microscope (SEM).

The Sb deposition efficiency (%) was calculated according to the equation below:

$$Sb\ deposition\ efficiencu\ (\%) = \frac{m_{experimental}}{m_{theoretical}} \times 100 \quad (14)$$

Where, m is the weight of deposited Sb for experimental and theoretical.

Furthermore, the theoretically expected amount of antimony was calculated according to the Faraday law given below:

$$m_{theoretical} = \frac{M x I x t}{z x F} \quad (15)$$

Where, M is the atomic mass of Sb (121.76 g/mol), I is the current in ampere, t is the time in seconds, z is the required electron number for one antimony atom (3 in our case), and F is the Faraday constant (96485 Coulomb).

On the other hand, consumed energy (E) during the electrolysis was calculated according to the equation given below:

$$E = V \times I \times t \quad (16)$$

Where, V is the Volt, I is the current in ampere, and t is time in hrs.

The specific energy consumption Es was calculated by:

$$E_S = \frac{E}{m_{deposited}} \quad (17)$$

Where, E is the energy consumed and m is the weight of deposited Sb.

Seven variables were determined to investigate the Sb deposition efficiency. These variables and their levels are represented in Table 2.

The additives to be used in the production of antimony by the electroproduction process were compared to determine the most suitable additive. These experimental series were carried out to compare the precipitating agents' effect on Sb deposition. For this context, $BaCl_2$, $CaCl_2$, $Ba(OH)_2$, and $Ca(OH)_2$ salts were selected as precipitating agents. The oxidation of antimony was prevented by precipitating agents occurring insoluble sulfate/sulfite salt of them during the electro-production process. The quantities corresponding to 48 and 96 mM of

Table 2. Variables of antimony deposition and their levels

Parameters	1	2	3	4
Sb (g/L)	15	25	35	45
NaOH (g/L)	100	200	300	400
Na_2S (g/L)	60	80	100	120
Time (hrs)	1	3	6	9
Cathodic Current Density (A/m^2)	47.6	95.2	-	-
Temperature (ºC)	25	40	55	70
Precipitating Agent Salt (mM)	0	24	48	96

each sample were weighed and added to the electrolysis cell.

4. Statistical Design

A traditional full factorial experiment design requires thousands of experiments if the number of parameters is high enough. On the other hand, the Taguchi experimental design is widespread and much easier to implement, especially for the optimization of experiments [23]. There are eight steps to performing the Taguchi experimental design. The first step is the selection of response variables to be optimized. The second step is the determination of parameters that affect the output variable. The third step is selecting a suitable orthogonal array in consideration of some of the parameters and levels of these parameters. The fourth step is to match the parameters with the selected orthogonal array. The fifth step is to perform the experiments. The final step is to analyze the results in consideration of signal-to-noise ratio (S/N) and to determine the impact of the various parameters. There are three calculation approaches for the Taguchi experimental design: "smaller-the-better", "nominal-the-better", and "larger-the-better". The most suitable levels of parameters are then determined. Finally, the confirmatory experiment is performed to determine if the analysis result is compatible with the real value [24]. All parameters except cathode current density had four levels. The cathode current density has two levels. Thus, an L32 mixed orthogonal array was selected to perform the experimental design. The main goal of the study was to achieve the highest Sb deposition efficiency. Thus, the S/N ratio was calculated according to the "the larger-the better" approach.

$$\frac{S}{N} = -log10\left[\frac{1}{n}\sum_{k=1}^{n}\frac{1}{y_k^2}\right]$$

Here, y_k represents the current efficiency value of the performed experiment, and n represents the total number of experiments (n=32). Minitab software [25]

was used for both the preparations of experimental design and the analysis of experimental results.

5. Results and Discussions

Before starting the Taguchi experimental setup, the precipitating agent effects on the Sb deposition were investigated in detail. A new process was designed to deposit Sb with environmentally friendly electro-extraction processes being non-corrosive and non-hazardous.

6. Comparison of Precipitating Agents

In this experimental series, each experiment was carried out at 25 °C for 3 hrs. and 47.6 A/m². The bath solution contained 25 g/L Sb, 100 g/L NaOH, and 80 g/L Na₂S. Stainless steel anode and cathode were used in all experiments. Experimental results are shown in Fig. 4. According to the results, the most promising additives were determined as $BaCl_2$, $Ba(OH)_2$, $CaCl_2$, and $Ca(OH)_2$, respectively.
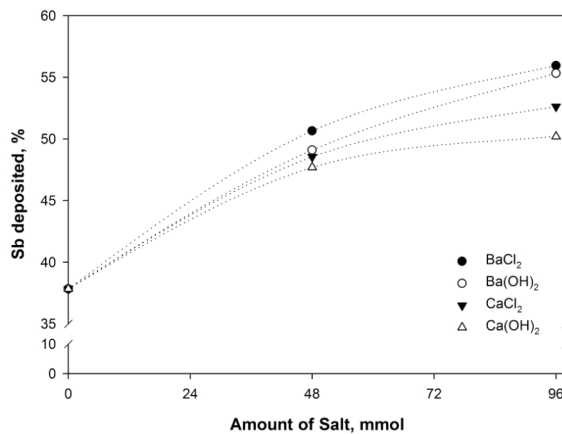

**Figure 4.** *Comparison of precipitating agents for antimony deposition*

As can be seen in Fig. 4, the barium salts appear to be more effective than the calcium salts. Considering the Ksp values given in Table 3, these results were expected. The determining factor is thought to be the difference in solubility product constant (K_{sp}) values between the precipitated hydroxide and sulfate compounds. The K_{sp} value of $Ba(OH)_2$ was greater than the K_{sp} value of $BaSO_4$. Since the pH level of the electrolyte was high (pH ≈ 14), $Ba(OH)_2$ precipitated first when $BaCl_2$ was added to the electrolyte, $Ba(OH)_2$ was already precipitated in experiments with $Ba(OH)_2$. A higher K_{sp} value of $Ba(OH)_2$ suggested that there were relatively more barium ions in the solution. Barium ions in solution were in sufficient quantity to form a $BaSO_4$ compound with oxidized sulfur ions on the anode surface. $Ba(OH)_2$ precipitate served as a source of barium during the electrolysis

process. During the electrolysis process, $Ba(OH)_2$ was depleted and transformed into $BaSO_4$ and $BaSO_3$. All of the final precipitate, formed as a result of the electrolysis process, consisted of $BaSO_4$ and $BaSO_3$. This result was confirmed by XRD analysis (see Fig. 10). On the other hand, the K_{sp} value of $Ca(OH)_2$ was relatively lower. This made it difficult to use $Ca(OH)_2$ as a source of calcium ions. However, the lower K_{sp} value of the $CaSO_3.0.5H_2O$ compound enabled the use of calcium hydroxide in antimony electrolysis. As seen in Fig. 4, calcium compounds also contributed to the increase in current efficiency, although not as much as barium compounds.

Table 3. *Ksp values of Compounds [18]*

Compound	K_{sp}
$BaSO_4$	1.08×10^{-10}
$BaSO_3$	5.0×10^{-10}
$Ba(OH)_2.8H_2O$	2.55×10^{-4}
$Ca(OH)_2$	5.02×10^{-6}
$CaSO_4$	4.93×10^{-5}
$CaSO_3.0.5H_2O$	3.1×10^{-7}

Another important finding seen in Fig. 4 is the contribution of chlorine ions to current efficiency. It is understood that chlorine-containing compounds are more effective in terms of current efficiency than hydroxide compounds of the related metal. $MeCl_2$ compound added to the solution with high pH precipitates as $Me(OH)_2$, Cl^- ion formed NaCl and remained in the solution. This caused an increase in the chloride ion concentration in the electrolyte. Thus, a new reaction was added to the possible oxidation reactions that may occur on the anode surface. This reaction is given in equation 18.

$$Cl^-_{(aq)} + 2OH^-_{(aq)} == OCl^-_{(aq)} + H_2O_{(l)} + 2e^-$$
$$E^0 = -0.89 \ V \tag{18}$$
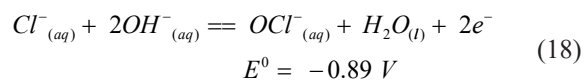
Chlorine gas, which is both harmful to the environment and causes corrosion of the anode, was expected to form because of the oxidation reaction of chloride ions. Therefore, the formation of chlorine gas was avoided in industrial applications. However, the reaction (Eq. 18) occurred in basic solutions instead of chlorine gas formation. This reaction reduced the likelihood of a sulfur oxidation reaction. Thus, chlorine ions indirectly contributed to the current efficiency by making the oxidation of sulfur difficult. In addition, it was worth mentioning that no corrosion was observed on the surface of the stainless-steel anodes used in the experiments. Considering all this, it was claimed that $BaCl_2$ was the most promising additive to be used in the antimony production alkaline bath by electroproduction process.

7. Analysis of Taguchi Experiments

The "the-larger-the-better" calculation method was chosen based on the Sb deposition efficiency. The current efficiency was calculated based on the ratio of the amount of deposited antimony to the amount of theoretical antimony deposition calculated by Faraday's law. All experiments were performed twice, and average results were recorded by Minitab Software [25] (see Fig. 5); the main effects plots for the S/N ratio graph were obtained from the results.

7.1. Effect of current density

In this study, 47.6 A/m^2 and 95.2 A/m^2 current densities were investigated. There were no significant differences between these two values. However, increasing the current density increased the coarseness of the deposition [26]. This phenomenon caused non-adherent structures to form on the cathode surface. For this reason, relatively low current densities should be chosen while performing the experiments.

7.2. Effect of Sb amount

The current efficiency was increased by increasing the antimony concentration as expected. A higher amount of antimony preferred the reduction of antimony ions to metallic antimony. Here, 25 g/L antimony was found to be unsuitable for electro-production production of antimony, which was in agreement with the literature. In contrast, precipitation of antimony in the form of Sb$_2$O$_3$ was observed when a higher Sb concentration was used, which was why the freshly prepared solution was used every time the experiment was performed. The solution should be kept continuously mixed while awaiting the experiment to prevent this precipitation.
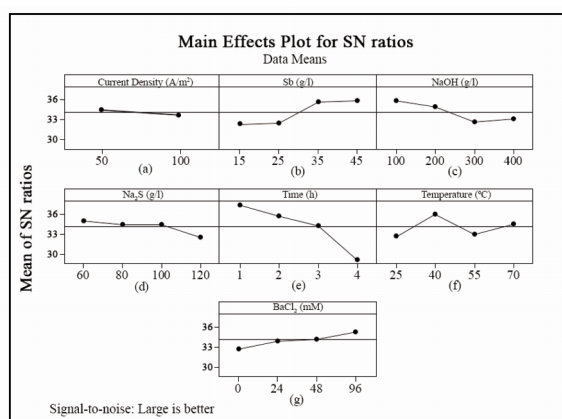

Figure 5. *(a): Effect of current denisty, (b); Effect of antimony amount, (c); Effect of NaOH amount, (d); Effect of Na$_2$S amount, (e) Effect of time, (f); Effect of temperature, (g); Effect of BaCl$_2$ concentration*

7.3. Effect of NaOH

According to the results seen in Fig. 5c, in the presence of BaCl$_2$, less NaOH was preferable for antimony production in terms of current efficiency. Increasing the amount of NaOH could prevent the oxidation of sulfur to higher stages and decrease the amount of precipitated BaSO$_4$ and BaSO$_3$ salts.

7.4. Effect of Na$_2$S

The higher amount of sulfur negatively affects the cathode current density as expected. As seen from Fig. 5d, the increasing amount of Na$_2$S had an adverse effect on the current efficiency. 60 g/L of Na$_2$S was chosen in the experiments. However, the presence of sulfur in alkaline antimony solutions was inevitable because Na$_2$S was both a suitable solvent for antimony compounds, and most antimony ores contained sulfur. The effect of Na$_2$S was investigated in detail in the next stage (see "effect of Na$_2$S and BaCl$_2$ addition").

7.5. Effect of time

Current efficiency decreased with increasing time. During electrolysis, the concentration of antimony naturally decreased because of metallic antimony deposition with time. The best results were obtained for 1 hr. according to the Taguchi experimental results (see Fig. 5e). However, refreshing the electrolyte every 1 hr. caused energy loss when applied industrially, and this was the reason why 3 hrs. of electro-deposition time was chosen for further experiments.

7.6. Effect of temperature

According to the experimental results, a temperature of 40 °C was the most effective temperature for the electro-production of antimony in the presence of BaCl$_2$. However, this result contradicted the literature. Increasing temperature resulted in an increment in the current efficiency for the electrowinning of antimony [27, 28] since the activation energy of the cathode reaction decreased. This result could suggest that higher temperatures increased the solubility of the barium salts, which then reduced the effect of barium ions.

7.7. BaCl$_2$ addition

The addition of a precipitating agent to the electrolyte made a significant contribution to the Sb deposition efficiency. The barium ions prevented the precipitation of the sulfide and sulfate ions generated from oxidized sulfur on the anode surface. Thus, the antimony ions (Sb^{+3}) were protected from oxidation

by sulfur-based ions. This finding encouraged the further optimization of the electro production process since the reaction could produce new chemical compounds such as barium sulfite or sulfate. This was an important advantage since barium sulfate was easily converted to barium carbonate to produce barium chloride at ambient conditions. Fig. 5g shows a linear correlation between the amount of $BaCl_2$ and the current efficiency. The effect of $BaCl_2$ was investigated in detail in the next stage (see "effect of Na_2S and $BaCl_2$ addition").

8. Confirmation Experiment

Table 4 shows the contribution of the parameters affecting the current efficiency of antimony deposition according to the Taguchi experimental design. Time is the most effective parameter in terms of Sb deposition efficiency. This means that changing the level of the time parameter makes a bigger difference in the current efficiency. In contrast, the current value had less effect on current efficiency.

As a result of Taguchi experiments, the most practical combination of levels was predicted in consideration of the "the-larger-the-better" strategy. Table 5 shows the levels of the parameters.

A new confirmation experiment was performed in two repetitions according to predicted values. At the end of the experiments, 0.22 g of antimony was deposited, which means that 96.9% of the Sb deposition efficiency was achieved; the values predicted by Taguchi analysis were confirmed by the experiment.

9. Effect of Na_2S and $BaCl_2$ addition

The effect of Na_2S and $BaCl_2$ was investigated in another experimental series to make a detailed observation. Parameters of 100 g/L NaOH, 40°C, 25 g/L Sb^{3+}, and 47.6 A/m^2 were chosen as constant parameters. Despite the best results obtained for 45 g/L of Sb^{3+}, a lower Sb concentration (i.e. 25 g/L of Sb^{3+}) was selected to observe the effect of both Na_2S and $BaCl_2$ concentration on the electro-production process. The second stage of experimental values is given in Table 6.

Table 5. *Response table for signal-to-noise ratios for "larger-is-better."*

Current (A/m^2)	Sb (g/L)	NaOH (g/L)	Na_2S (g/L)	Time (h)	Temperature (°C)	$BaCl_2$ (mM)
47.6	45	100	60	1	40	960

Table 6. *Second stage experimental values*

Exp No	1	2	3	4	5	6	7	8	9	10	11	12	13	14	15	16
Na_2S (g/L)	60				80				100				120			
$BaCl_2$(mM)	0/24/48/96				0/24/48/96				0/24/48/96				0/24/48/96			

According to Fig. 6, the negative effect of Na_2S was observed. Expectedly, the amount of Na_2S linearly decreased the antimony deposition without $BaCl_2$. At this condition, approximately 0.55 g of Sb was deposited in the presence of 60 g/L Na_2S and the deposited Sb efficiency was also found at 81.5%.

In the following experiments without $BaCl_2$, the decreasing trend was observed when increasing the Na_2S content up to 120 g/L. The lowest deposition was recorded at around 0.18 g of Sb with 26% a Sb deposition. To understand the effect of $BaCl_2$ addition, three different concentrations (i.e. 24, 48, and 96 mM) of $BaCl_2$ were investigated with changes of Na_2S concentration. The addition of $BaCl_2$ had an interesting positive effect on collected Sb quantities,
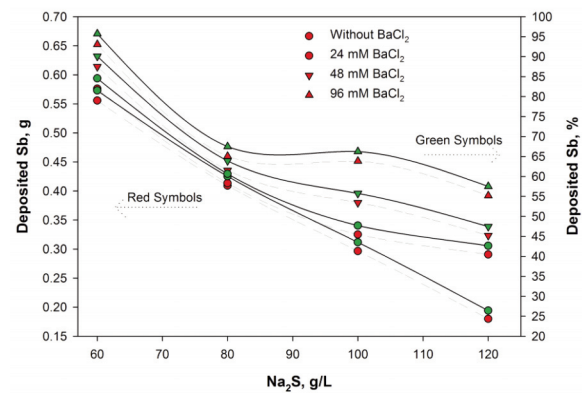
Figure 6. *Deposited Sb as a function of Na_2S and $BaCl_2$ quantity*

Table 4. *S/N ratio values predicted by Taguchi Experimental Design*

Level	Current Density	Sb (g/L)	NaOH (g/L)	Na_2S (g/L)	Time (h)	Temperature (°C)	$BaCl_2$ (mM)
1	34.65	32.75	35.83	35.01	37.48	32.78	157.6
2	33.66	32.28	34.99	34.50	35.71	36.04	163.8
3		35.66	32.59	34.44	34.24	33.04	164.5
4		35.78	33.05	32.51	29.03	34.61	169.5
Delta	0.92	3.5	3.23	2.5	8.44	3.26	2.49
Rank	7	2	4	5	1	3	6

as well as Sb deposit percentage. Here, 24 mM $BaCl_2$ addition slightly prevents the harmful effect of sulfide ions on Sb deposition. It was concluded that the presence of $BaCl_2$ suppressed the negative effect of the sulfate ion. A 95.7% Sb deposition efficiency was attained in the presence of 96 mM (i.e. 20 g/L) $BaCl_2$, in the bath containing 60 g/L Na_2S. However, the lowest Sb deposition efficiency was achieved in the presence of 120 g/L Na_2S. Similarly, for the experiments performed with 120 g/L Na_2S, the Sb deposition percentage increased from 26% to above 57% (around twofold) in the presence of 96 mM $BaCl_2$.

Fig. 7 shows the voltage change during the electro-deposition process. Experiments No.3 and 4 were chosen to demonstrate the effect of the addition of $BaCl_2$ on the polarization of the electro-production process. Both experiments were performed under the same conditions, i.e. 40 °C, 100 g/L NaOH, and 60 g/L Na_2S, and 47.6 A/m², 3 hrs.

The main difference between the two experiments was the amount of $BaCl_2$, which was 48 and 96 mM, respectively. Both experiments showed similar fluctuating voltage changes. The average voltage changes of exp. 3 # and exp. 4 # were 1.85 V and 1.99 V, respectively. The average voltage difference between the two experiments was approximately 140 mV. This voltage decrease was probably caused by the removal of oxidized sulfur species, which were concurrently precipitated by barium ions.

On the other hand, the energy consumption of metallic antimony production could be deduced from Fig. 7. The areas under the lines were directly proportional to energy consumption. Accordingly, energy consumption in exp. 3 # and exp. 4 # was 0.833 J and 0.896 J, respectively. Besides, specific energy consumption values could be generated from energy consumption values and the amount of deposited antimony, which were 0.614 g for exp. 3 and 0.652 g for exp. 4, respectively. The specific

energy consumption of exp. 3# containing 48 mM $BaCl_2$ was 2.19 kWh/kg. The specific energy consumption of experiment 4 containing 96 mM was 1.99 kWh/kg. These results revealed that increasing the amount of $BaCl_2$ decreased the energy consumption per 1 kg of deposited metallic antimony.

10. Kinetics Mechanism of Antimony Electro-production

In the kinetic analysis of the electro-production process, the voltage-current density graph was drawn as seen in Fig 8. According to this figure, it was observed that the current started to occur after applying 0.5 volts to the stainless-steel cathode surface. Alternatively, the experiment was repeated using the antimony-coated cathode. In this case, the voltage at which the current started to occur was observed as 1.1 V.

This indicates that the reduction of sulfur at the antimony surface requires more voltage. This phenomenon is called "sulfur overvoltage" on stainless-steel surfaces. Just like in the present study, the choice of the cathode is important in the production of antimony from alkaline solutions by the electro-production process. However, when the antimony completely covered the cathode surface, the quality of the cathode became insignificant. In addition, when the voltage-current density graph was examined, it was seen that the limiting current density value had not been reached. It is known that limiting current occurs in diffusion-controlled processes. The density of the cations to be reduced in the region called the Nernst layer on the cathode surface comes to the minimum level. This occurs when the reduction rate is greater than the diffusion rate at higher voltages. In such cases, it is called "diffusion control" since the mechanism with the slower rate is decisive. To provide a diffusion-controlled reaction, the number of unreacted cations on the cathode surface should be relatively high. Although there were unreacted Ba^{2+}
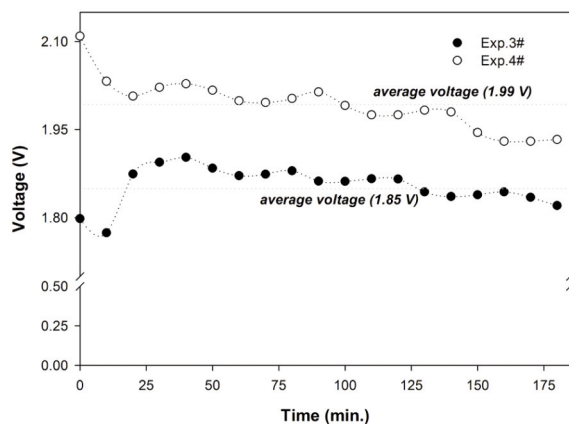

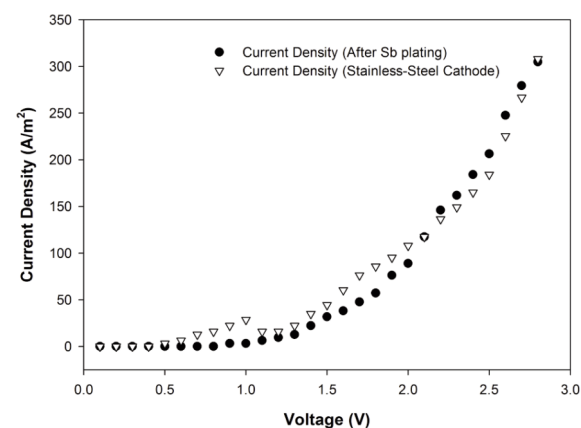***Figure 7.*** *Voltage changes during experiments No:3 and 4 as function a time*

Figure 8. *Current density changes as a function of voltage*

and Na^+ cations in the solution, the amounts of these cations were not sufficient for the diffusion-controlled reaction. In light of these findings, the Tafel plot was drawn from the current density versus voltage graph (i.e., Fig. 9). The electro-production process was compared with one another in the absence/presence of $BaCl_2$.
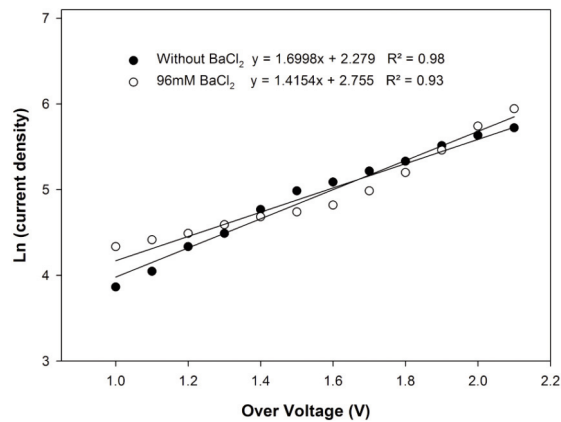

Figure 9. Tafel Plot

According to the Tafel plot, the slope of the line formed by the experiment containing $BaCl_2$ was found to be 1.4154, and the slope of the line formed by the experiment without $BaCl_2$ was found to be 1.6998. By extrapolating the Tafel lines, the exchange current density values were calculated through the logarithmic current density values corresponding to the 0-volt over-voltage value (equilibrium state). The point where the Tafel line of the experiment with 96 mM $BaCl_2$ intersected with the y-axis was 2.755; the point where the Tafel line of the experiment without addition intersects with the y-axis is 2.279. Considering these values, the exchange current density value of the electrolysis process containing $BaCl_2$ was calculated as 15.72 A/m^2, and the exchange current density value of the electrolysis process without additives was calculated as 9.776 A/m^2.

The reduction of sulfur cations is a homogeneous reaction. The reactants and products of the reaction are in the same phase. On the other hand, the reduction of antimony is a heterogeneous reaction. Antimony cations in the aqueous phase pass into the solid phase after reduction. In equilibrium, homogeneous reactions occur more easily than heterogeneous reactions. Therefore, a lower exchange current density was expected for homogeneous reactions compared to heterogeneous reactions since two electrons were involved in a homogenous reaction and three electrons were involved in a heterogeneous reaction. As a result, the increase in exchange current density with the addition of $BaCl_2$ was an indication that the efficiency of sulfur had

decreased. In other words, it was proved by the obtained Tafel plot that the addition of $BaCl_2$ made the reduction of sulfur difficult on the cathode surface, as claimed.

11. Characterization of powders

After the electro-production process was completed, the electrolyte solution was filtered. Afterward, the precipitated residue was rinsed several times with distilled water and dried in a vacuum desiccator to carry out the analysis via XRD. The XRD results are presented in Fig. 10. It is known that the current efficiency is dependent on the formation of barium sulfide and barium sulfate salts because these salts have almost no solubility in the solution, which in turn increases the current efficiency due to the elimination of oxidized sulfur species.
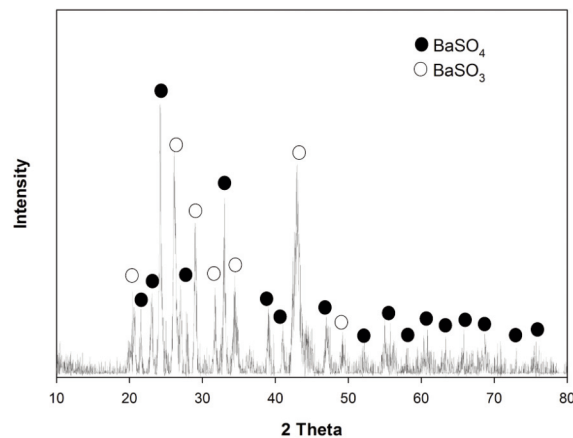

Figure 10. The XRD results of the precipitated powder in the bath

The XRD result showed that the major phase of the residue was $BaSO_4$. The minor phase was found to be $BaSO_3$, which ment that oxidized sulfur compounds were precipitated with barium ions. Increasing the current efficiency owing to the presence of barium ions proved that sulfur ions were removed from the electrolyte before the oxidation of antimony to further oxidation step.

Figure 11a, 11b, and 11c display the XRF and XRD patterns and SEM images of the produced metallic antimony, respectively.

Both XRF and XRD patterns proved that the produced product was metallic antimony. The SEM image of the produced metallic antimony was presented in Fig.11c. It was seen from the SEM image that antimony had accumulated spherically on the cathode surface and the size of the formed grains varies between 200 nm and 400 nm.
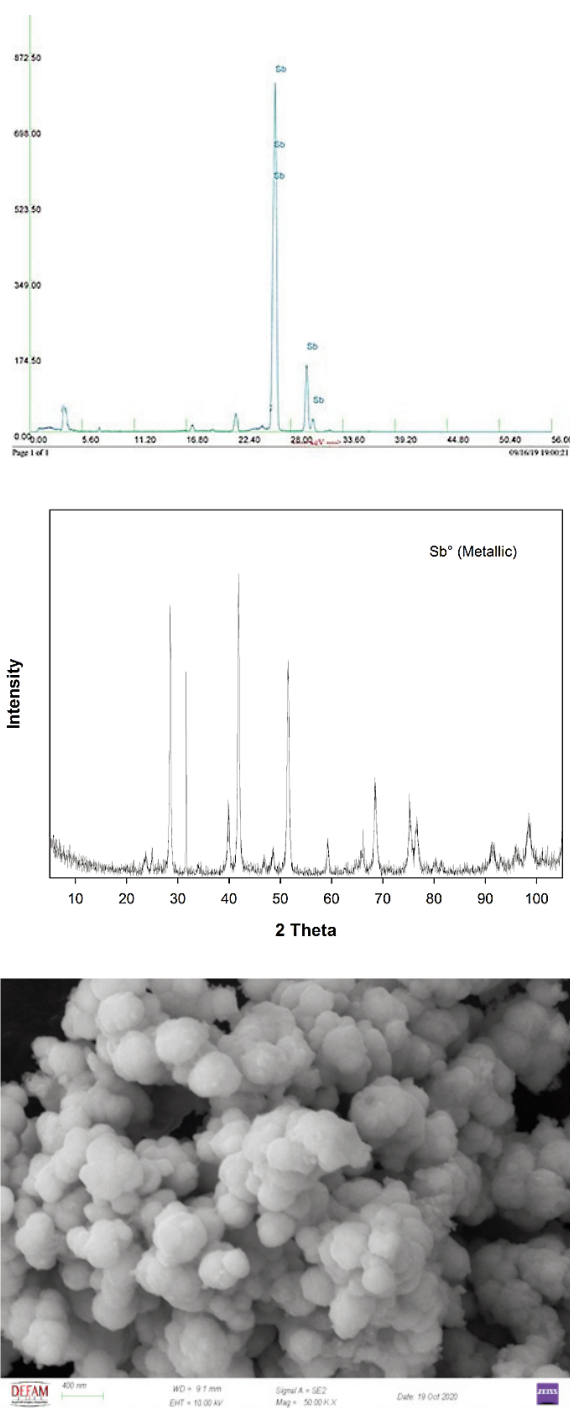
Figure 11. The characterization of the produced metallic antimony using XRF, XRD, and SEM

12. Conclusion

The major problem of antimony production by electrolysis is the efficiency loss caused by the oxidized sulfur ions. The present study covered the electro-production of antimony via non-diaphragm cells. The use of precipitating agents was inspired by a previously published patent to overcome this problem. Various precipitating agents (i.e., $BaCl_2$, $CaCl_2$, $Ba(OH)_2$, $Ca(OH)_2$) were used in this context to precipitate the oxidized sulfur ions in order to increase current efficiency and determine Sb deposition quantity. The highest Sb deposition was found in $BaCl_2$ salt. Factors that affected current efficiency were optimized via the Taguchi experimental design method. For example, 45 g/L Sb, 100 g/L NaOH, and 60 g/L Na_2S concentrations were determined as the most optimum values for antimony production; 40°C was determined as the most efficient temperature for electro-production in the presence of Ba^{2+}. Furthermore, the current efficiency decreased with increasing time, in line with the scientific literature [22], and the XRD result of the precipitated powder in the bath showed that oxidized sulfur ions were precipitated by $BaCl_2$.

The results showed that $BaCl_2$ had a positive effect on the current efficiency in that an increasing amount of $BaCl_2$ led to an increase of 31.1% in the current efficiency. However, this effect was more profound if the electrolyte contained a higher concentration of sulfur ions. Na_2S was an efficient solvent for antimony compounds, and most antimony ores contained sulfur, so that $BaCl_2$ could be successfully employed as a precipitation agent during electro-production. In the case of lower sulfur concentrations, it was recommended that $BaCl_2$ addition could also be used to enhance the current efficiency with other applications such as increasing the anodic current density. Here, $BaSO_4$ and $BaSO_3$ salts were obtained as side products. For industrial applications, these salts were recommended to be converted back to $BaCl_2$. Several studies are published in the literature regarding the conversion of barium sulfate to barium chloride. Recently, barite ($BaSO_4$) ore can be easily converted to barium carbonate to produce other compounds of barium.

At 10 g/L $BaCl_2$, the specific energy consumption was 2.19 kWh/kg, and at 96 mM $BaCl_2$, it was 1.96 kWh/kg. These results revealed that increasing the amount of $BaCl_2$ caused a decrease in energy consumption per 1 kg of deposited metallic antimony. Further study for producing antimony metal, the calculation of the economic balance may show how the improvement is important to the process.

Author contributions

M. H. Morcali and S. Aktaş conceived and designed the study. Ö. Küçükoğlu performed the experiments. Ö. Küçükoğlu, M. H. Morcali and B. N. Cetiner wrote the manuscript. M. H. Morcali and S. Aktaş reviewed and edited the manuscript. All authors read and approved the manuscript.

Conflict of Interest

On behalf of all authors, the corresponding author states that there is no conflict of interest.

References

[1] S. Dembele, A. Akcil, S. Panda, Technological trends, emerging applications and metallurgical strategies in antimony recovery from stibnite, Minerals Engineering, 175 (2022) 107304. https://doi.org/10.1016/j.mineng.2021.107304.

[2] L. S. Martins, L. F. Guimarães, A. B. B. Junior, J. A. S. Tenório, D. C. R. Espinosa, Electric car battery: An overview on global demand, recycling and future approaches towards sustainability, Journal of Environmental Management, 295 (2021) 113091. https://doi.org/10.1016/j.jenvman.2021.113091

[3] L. Grandell, A. Lehtilä, M. Kivinen, T. Koljonen, S. Kihlman, L. S. Lauri, Role of critical metals in the future markets of clean energy technologies, Renewable Energy, 95 (2016) 53-62. https://doi.org/10.1016/j.renene.2016.03.102.

[4] E. C. Giese, Strategic minerals: Global challenges post-COVID-19, The Extractive Industries and Society, (2022) 101113. https://doi.org/10.1016/j.exis.2022.101113.

[5] EU_CRM_Report. Study on the EU's list of Critical Raw Materials. 2021 [cited 2021 01 October]; Available from: https://rmis.jrc.ec.europa.eu/uploads/CRM_2020_Report_Final.pdf.

[6] C.G. Anderson, The metallurgy of antimony, Geochemistry, 72 (2012) 3-8. https://doi.org/10.1016/j.chemer.2012.04.001.

[7] D. Dupont, S. Arnout, P. T. Jones, K. Binnemans, Antimony recovery from end-of-life products and industrial process residues: A critical review, Journal of Sustainable Metallurgy, 2 (1) (2016) 79-103. https://doi.org/10.1007/s40831-016-0043-y.

[8] F. Habashi, Handbook of extractive metallurgy, Wiley-VCH, Quebec, 1997: p. 280.

[9] C. G. Anderson, S. M. Nordwick, L. E. Krys, Antimony separation process, US 5290338A (1992)

[10] Q. Wang, Y. Wang, Fundamental electrochemical behavior of antimony in alkaline solution, Journal of Sustainable Metallurgy, 5 (4) (2019) 606-616. https://doi.org/10.1007/s40831-019-00253-7.

[11] M. K. Carpenter, M. W. Verbrugge, Electrochemical codeposition of indium and antimony from a chloroindate molten salt, Journal of Materials Research, 9 (10) (1994) 2584-2591. https://doi.org/10.1557/JMR.1994.2584.

[12] R. K. Iyer, S. G. Deshpande, Preparation of high-purity antimony by electrodeposition, Journal of Applied Electrochemistry, 17 (5) (1987) 936-940. https://doi.org/10.1007/BF01024359.

[13] R. S. Multani, T. Feldmann, G. P. Demopoulos, Antimony in the metallurgical industry: A review of its chemistry and environmental stabilization options, Hydrometallurgy, 164 (2016) 141-153. https://doi.org/10.1016/j.hydromet.2016.06.014.

[14] W. Liu, T.-z. Yang, Q.-h. Zhou, D.-c. Zhang, C.-m. Lei, Electrodeposition of Sb(III) in alkaline solutions containing xylitol, Transactions of Nonferrous Metals Society of China, 22 (4) (2012) 949-957. https://doi.org/10.1016/S1003-6326(11)61269-7.

[15] P. Raschman, E. Sminčáková, Kinetics of leaching of stibnite by mixed Na2S and NaOH solutions, Hydrometallurgy, 113-114 (2012) 60-66. https://doi.org/10.1016/j.hydromet.2011.11.017.

[16] J.-g. Yang, Y.-t. Wu, A hydrometallurgical process for the separation and recovery of antimony, Hydrometallurgy, 143 (2014) 68-74. https://doi.org/10.1016/j.hydromet.2014.01.002.

[17] J. C. Jiménez-Lugos, R. G. Sánchez-Alvarado, A. Cruz-Ramírez, J. A. Romero-Serrano, A. Hernández-Ramírez, J. E. Rivera-Salinas, Antimony recovery from recycled terminals of lead-acid batteries with Na2CO3 and SiC after the formation of Sb2O3, Journal of Mining and Metallurgy, Section B: Metallurgy, 58 (1) (2022) 97-108. https://doi.org/10.2298/JMMB210616052J.

[18] R. H. Petrucci, General chemistry: principles and modern applications, Pearson, New York, 2017 p.345.

[19] W. C. Holmes Electrolytic recovery of metals, US 2331395A (1940)

[20] N. F. R. Lindstrom Method for the electrolytic recovery of Sb, As, Hg and/or Sn, US 4017369A (1975)

[21] S. A. Awe, Å. Sandström, Electrowinning of antimony from model sulphide alkaline solutions, Hydrometallurgy, 137 (2013) 60-67. https://doi.org/10.1016/j.hydromet.2013.04.006.

[22] S. A. Awe, J.-E. Sundkvist, Å. Sandström, Formation of sulphur oxyanions and their influence on antimony electrowinning from sulphide electrolytes, Minerals Engineering, 53 (2013) 39-47. https://doi.org/10.1016/j.mineng.2013.07.001.

[23] J. L. Rosa, A. Robin, M. B. Silva, C. A. Baldan, M. P. Peres, Electrodeposition of copper on titanium wires: Taguchi experimental design approach, Journal of Materials Processing Technology, 209 (3) (2009) 1181-1188. https://doi.org/10.1016/j.jmatprotec.2008.03.021.

[24] M. S. Phadke, Quality engineering using robust design, Prentice Hall PTR, New Jersey, 1995 p. 285-301.

[25] MiniTab. MiniTab Software. 2021 [cited 2021 5 Oct]; Available from: https://www.minitab.com/en-us/products/minitab/free-trial/.

[26] K. I. Popov, S. S. Djokić, N. D. Nikolić, V. D. Jović, Morphology of electrochemically and chemically deposited metals, Springer, Belgrade, 2016 p.201.

[27] A. Wikedzi, Å. Sandström, S. A. Awe, Recovery of antimony compounds from alkaline sulphide leachates, International Journal of Mineral Processing, 152 (2016) 26-35. https://doi.org/10.1016/j.minpro.2016.05.006.

[28] S. M. Moosavi Nejad, The effect of temperature on the electrowinning of antimony from alkaline sulfide solution, Journal of Advanced Materials and Technologies, 9 (4) (2021) 47-58. https://doi.org/10.30501/jamt.2021.238557.1102

ELEKTRODEPOZICIJA ANTIMONA BEZ DIJAFRAGME: UTICAJ PARAMETARA PROCESA I SREDSTAVA ZA TALOŽENJE

M.H. Morcali [a*], Ö. Küçükoğlu [b,c], B.N. Çetiner [b], S. Aktaş [b]

[a] Srednja stručna škola Naci Topcuoglu, Univerzitet u Gazijantepu, Gazijantep, Turska
[b] Fakultet za metalurgiju i inženjerstvo materijala, Univerzitet Marmara, Istanbul, Turska
[c] Univerzitet Beykent, Fakultet za mehaniku, Esenyurt/İstanbul, Turska

Apstrakt

Proizvodnja metalnog antimona iz materijala koji sadrži antimon je jedna od najistraživanih tema u ovoj oblasti. Konvencionalna tehnologija dobijanja antimona elektrolizom predstavlja izazovan problem zbog jedinjenja sumpora koja potiču iz same rude i iz rastvora za luženje u sistemu elektrolize. : Elektro-proizvodnja antimona u modifikovnim ćelijama bez dijafragme je od interesa jer ćelije koje sadrže dijafragme imaju probleme sa održavanjem i visoku cenu koštanja.
U fokusu ovog istraživanja je bio problem sumpora u ćelijama bez dijafragme i zbog toga su ispitivani efekti različitih soli na ovaj problem, a uslovi proizvodnje antimona su optimizovani. Kao taložni agens za formiranje nerastvorljivih soli ($BaSO_4/CaSO_4$ i $BaSO_3/CaSO_3$) korišćene su različite soli (tj. $BaCl_2$, $CaCl_2$, $Ba(OH)_2$, $Ca(OH)_2$). Koncentarcija Sb, količina NaOH i Na_2S, vreme ekstrakcije elektrolizom i temperatura ispitivani su kako bi se optimizovali reakcioni parametri. Korišćen je Taguči eksperimentalni dizajn za određivanje uticaja svakog faktora na taloženje Sb. Faze i strukture nastale tokom elektro-proizvodnje identifikovane su uz pomoć različitih tehnika merenja. Istraživanje je pokazalo da su u prisustvu 96 mM $BaCl_2$, 45 g/L koncenntracije Sb, 100 g/L NaOH i 60 g/L Na_2S faktori bili najpogodniji za postupak. Utvrđeno je da je 40 °C optimalna temperatura za ekstrakciju elektrolizom. Ovaj rezultat je takođe pokazao da povećanje koncentracije $BaCl_2$ smanjuje specifičnu potrošnju energije.

Ključne reči: Antimon; Elektrohemijski proces; Metalne soli; Taloženje